

# On Modeling and Personal Dosimetry of Cellular Telephone Helical Antennas with the FDTD Code

Gianluca Lazzi, *Member, IEEE*, and Om P. Gandhi, *Fellow, IEEE*

**Abstract**— In this paper, a novel method to model helical antennas working in the normal mode, as well as helix-monopole antennas with finite-difference time-domain (FDTD) code is presented. This method is particularly useful to model antennas used for personal wireless communication handsets, where the fairly small dimensions of the helical antennas with respect to wavelength and the grid cell size do not allow an appropriate description of the antennas by the use of metal wires. By observing that a helix working in the normal mode is equivalent to a sequence of loops and dipoles, it is possible to model the helix as a stack of electric and magnetic sources with relative weights calculated using information obtained from analytical expressions for the far-fields. Dosimetry associated with wireless telephones using helical antennas is then considered by calculating the specific absorption rates (SAR's) induced by two actual devices in a  $1.974 \times 1.974 \times 3.0$ -mm resolution model of the human head based on MRI scans of a male volunteer. Comparison of the computed results with experimental measurements in the near field, the far field, and the induced SAR's shows good agreement.

**Index Terms**— FDTD methods, land mobile radio cellular systems, radiation effects.

## I. INTRODUCTION

IN the last few years, an ever-increasing effort has been made to improve the characteristics of antennas for mobile telephones. A requirement is to develop antennas of smaller dimensions without significant reduction of performance. There is, therefore, a great interest at the present time in the relatively shorter helical antennas that can reduce considerably the length of the antenna, while providing radiation characteristics that are comparable to longer monopole antennas. For mobile telephones these antennas function in the so-called “normal mode,” i.e., the maximum radiation is in a plane normal to the orientation of the antenna. Such a radiating mode has been studied in the literature [1]. It has been shown that for situations where the physical dimensions of the antenna (diameter and length) are much smaller than the wavelength, the helix can be approximated by a series of small loops and dipoles having diameter equal to the diameter of the helix and length equal to the pitch of the helix, respectively.

Since it allows inclusion of anatomically based head models, the finite-difference time-domain method (FDTD) [2]–[5] is currently the most used computational methods to calculate the rates of electromagnetic energy absorption [specific absorption rates or (SAR's)] in the human head due to cellular telephones

[6]–[9]. The modeling of increasingly popular helical antennas has generally not been addressed in the literature even though it is possible to find alternative approaches that consider the model of thin loops and dipoles [10].

In this paper, we make use of the observation that the helix is equivalent to a series of loops and dipoles [1] and model it as a set of electric and magnetic sources with relative magnitudes calculated using the analytical expressions of the far fields. Special attention is given to properly place these sources in order to obtain a good agreement with measurements also in the near-field region.

Two typical cellular telephones have been used: one with helix antenna and one with helix-monopole antenna; measurements of the far fields as well as the near fields show the reliability of this approach. These telephones have also been tested against the ANSI/IEEE Safety Guidelines [11] that prescribe a maximum SAR of 1.6 W/kg averaged over any 1 g of tissue. The results given by the FDTD simulations were compared with the measured results obtained by the use of the Utah heterogeneous experimental model. A good agreement between measured and computed SAR's has been found.

## II. THE MODELING OF THE HELIX

A small diameter (compared to wavelength) helix antenna working in the normal mode and a series of equivalent loops and dipoles are shown in Fig. 1(a) and (b), respectively. As in [1], the far field can be calculated, therefore, considering as source only one loop and one dipole. Defining  $\eta$  as the characteristic impedance and  $k$  the propagation constant of the free-space, we can write

$$E_\theta(r) = j\eta k I_d S \frac{\sin \theta}{4\pi r} e^{-jk r} \quad (1)$$

$$E_\phi(r) = \eta k I_l S \frac{\pi^2 D^2}{2\lambda} \frac{\sin \theta}{4\pi r} e^{-jk r} \quad (2)$$

where, according to Fig. 1(a),  $D$  is the diameter of the helix,  $S$  is the pitch, and  $I_d$ ,  $I_l$  are the currents passing, respectively, through the dipole and the loop.

Therefore, in the far field we have

$$\frac{E_\theta}{E_\phi} = j \frac{I_d}{I_l} \frac{2S\lambda}{\pi^2 D^2} = j \frac{2S\lambda}{\pi^2 D^2} \quad (3)$$

because of the continuity of the current  $I_d = I_l$ .

The objective now is to relate the ratio that one obtains from (3) to the sources to prescribe for the FDTD. Referring to Fig. 1(b) where the dipole is placed along the  $z$  direction with the axis of the loop in the same direction, we can write

Manuscript received August 22, 1996; revised December 16, 1997.

The authors are with the Department of Electrical Engineering, University of Utah, Salt Lake City, UT 84112, USA.

Publisher Item Identifier S 0018-926X(98)02679-9.

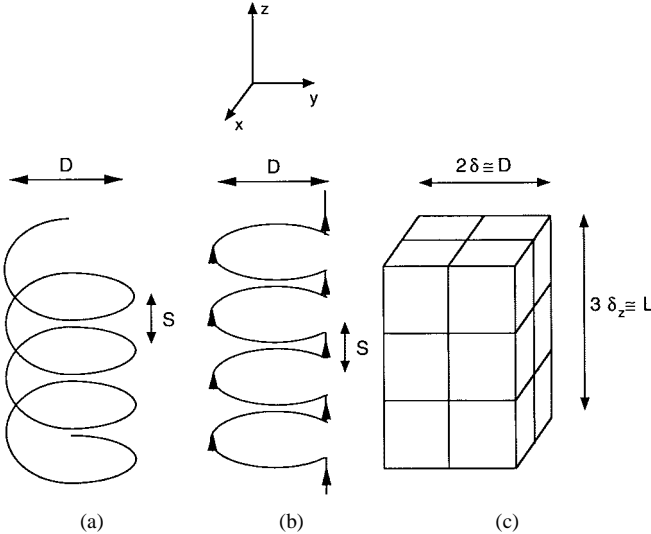


Fig. 1. (a) The equivalence of a “normal-mode” helix antenna. (b) A sequence of loops and dipoles [1]. (c) The FDTD cells along the  $x$ ,  $y$ , and  $z$  directions used to model the helix.

an equivalent electric field  $E_z$  for a single FDTD cell in lieu of the current  $I'_d$  in the dipole. Assuming for simplicity equal cell size  $\delta$  in the  $x$  and  $y$  direction, we can write

$$E_z = I'_d \frac{1}{j\omega\epsilon_0\delta^2}. \quad (4)$$

Furthermore, the magnetic field in the  $z$  direction related to the current  $I'_l$  due to a loop in the same grid cell can be expressed by [12]

$$H_z = I'_l \frac{1}{2\frac{\delta}{2}} = I'_l \frac{1}{\delta}. \quad (5)$$

For a single FDTD grid cell we, therefore, have

$$\frac{E_z}{H_z} = \frac{I'_d}{I'_l} \frac{1}{j\omega\epsilon_0\delta}. \quad (6)$$

Because the dipole- and loop-equivalent sources need to conform to the FDTD grid size, the respective currents  $I'_d$  and  $I'_l$  need to be defined accordingly. These currents need to be related to the currents  $I_d$ ,  $I_l$  produced by the actual dipole and loop. We found that good results are obtained by scaling the dipole current by the ratio of the actual and the modeled dipole lengths and the loop current by the ratio of the actual and the modeled loop perimeters. Defining  $a = D/2$ , and indicating with  $\delta_z$  the cell size in the  $z$  direction, we can write

$$I'_d = I_d \frac{S}{\delta_z} \quad (7)$$

$$I'_l = I_l \frac{2\pi a}{4\delta} = I_l \frac{\pi a}{2\delta}. \quad (8)$$

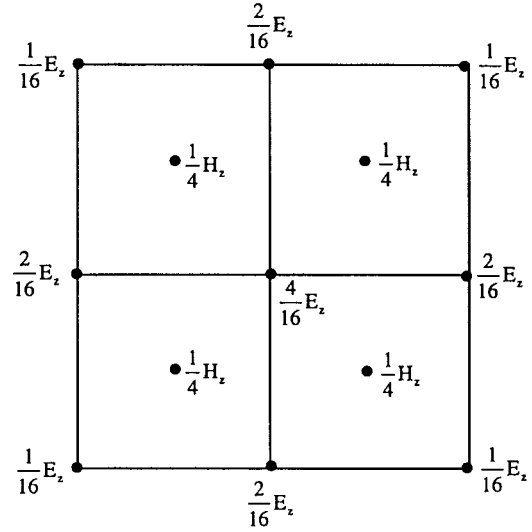


Fig. 2. The excitation method for one layer “ $x$ - $y$ ” of the stack of cells along the  $z$  direction used to model the helix.

Equation (6) can, therefore, be rewritten as

$$\frac{E_z}{H_z} = \frac{I_d}{I_l} \frac{2S}{j\omega\epsilon_0\pi a\delta_z} = \frac{2S}{j\omega\epsilon_0\pi a\delta_z} \quad (9)$$

since  $I_d = I_l$ .

### III. IMPLEMENTATION OF THE FDTD

Before modeling the helix in the actual FDTD code, it has usually been necessary to run a short simulation with the excitation prescribed by (9) to determine whether it is possible to obtain the ratio  $E_\theta/E_\phi$  in the far fields that is given by (3). It has been found that corrections  $E_z/H_z$  on the order of 10% may be necessary to obtain a better match to the ratio  $E_\theta/E_\phi$  in the far field given by (3). Particularly, in this simulation an electric source and a magnetic source are excited in the same cell in order to simulate the presence of one dipole and one loop with a ratio given by (9). Furthermore, to take into account the 90° phase difference between  $E_z$  and  $H_z$ , the two sources should be excited with sinusoidal and sinusoidal waveforms, respectively.

To better match to the physical dimensions of the helix and obtain a near field closer to the actual one, the helix has been modeled by splitting the excitation with electric and magnetic fields along the  $x$ ,  $y$ , and  $z$  directions. Fig. 1(c) depicts this excitation method for the case where to represent the helix four cells are necessary in the  $x$ - $y$  planes and three cells along the  $y$ - $z$  and  $x$ - $z$  planes. The number of sources in the  $z$  direction, i.e., along the axis of the helix, should be chosen to match the total length  $L$  of the helix. In the  $x$ - $y$  plane, instead, the number of source cells should be such as to have an area as close as possible to that of the helix.

As illustrated in Fig. 2, to split the sources in the  $x$ - $y$  plane, the number of cells that have a common corner is considered. In particular, the relative electric field as calculated by (9) should be divided amongst all the cells in the  $x$ - $y$  plane chosen to represent the helix. If a corner is common to four cells, the

TABLE I  
DIMENSIONS OF THE CONSIDERED TELEPHONES  
AND PARAMETERS USED FOR THE SIMULATIONS

Telephone	Freq. (MHz)	Box Dimensions x, y, z (cm)	Helix dimensions Diam., Pitch, Length (mm)
A	1900	2.2, 5.6, 15.6	5, 4.5, 17
B	835	2.4, 5.2, 14.7	4.2, 1.4, 16
C	1900	2.5, 5.0, 15.0	5, 2.5, 14

value of the electric field in that location is set to be four times the value assumed in a corner belonging to just one cell. Similarly, if a corner is common to two cells, the value of the electric field will be twice the value assumed in a corner belonging to a single cell.

The required magnetic field  $H_z$ , instead, is simply divided in equal parts amongst the four cells. This is because the magnetic field is excited in the center of each cell and, therefore, the assigned values should not take into account an “overlap” of excitations. Fig. 2 describes this excitation method for one  $x$ - $y$  plane of the stack of cells used to model the helix.

The excitations thus split (Fig. 2) should be repeated for all the layers along the  $z$  direction used to simulate the helix. Not knowing the current distribution along this axis, an interesting issue has been how to prescribe the relative magnitudes of the excitations in the axial direction of the helix. To resolve this issue, we started with three assumed distributions in the axial direction, i.e., uniform, and one quarter and one half of a sinusoidal variations of  $E_z$  and  $H_z$  prescribed for the axial direction. The final current distribution along the  $z$  direction was obtained using the equation

$$I = \oint \vec{H} \cdot d\vec{l}. \quad (10)$$

As a result, we found that the effect of weighting along the  $z$  axis is fairly independent of the shape of the weighting function. A representative example of this is shown in Fig. 3, where the current distribution as obtained from (10) is given for a helix mounted over a metal box. The telephone and antenna parameters used in the simulation are as given for telephone A in Table I. The helix is placed at the center position with respect to the  $x$  axis, and 4 mm from the right-hand side with respect to the  $y$  axis (see the insert of Fig. 3). The FDTD grid resolution for this test case, as well as for the other cases presented in the paper, was  $1.974 \times 1.974 \times 3$  mm in the  $x$ ,  $y$ , and  $z$  directions, respectively. Therefore, a stack of six layers, each one composed of four source cells, has been chosen to represent this helix.

#### IV. RESULTS

As a first comparison with helical antennas typically used for wireless devices, we considered the far fields generated by a cellular telephone. The dimensions of the telephone are

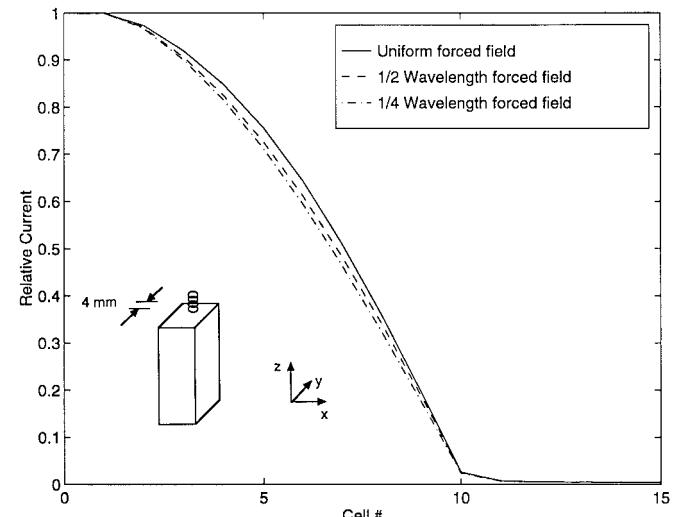


Fig. 3. The calculated current distribution along the axis of a helical antenna placed above a metal box. Uniform and one quarter and one half of a sinusoidal variation are assumed for the excitations  $E_z$  and  $H_z$ . Box dimensions:  $2.2 \times 5.6 \times 15.6$  cm. The helix placed as shown in the insert has diameter  $D = 5$  mm, pitch  $S = 4.5$  mm, length  $L = 1.7$  cm. Frequency: 1900 MHz.

given in Table I (telephone B) and the helix is mounted on the right-hand corner on the distal side with respect to the side of the earphone. The telephone has been modeled by a metal box covered with plastic of thickness 1 mm with a dielectric constant  $\epsilon_r = 4$ . As discussed in [6], this is scaled to match with the FDTD grid resolution ( $1.974 \times 1.974 \times 3$  mm), which results in an effective dielectric constant  $\epsilon_{\text{eff}} = 1.6$ . Particular attention has been given to the modeling of the base of the actual helix, which also included a straight metal connection above the box of 2 cm.

The calculated radiation pattern in the  $x$ - $y$  plane has been compared to that provided by the manufacturer and it is shown in Fig. 4 in dBi. Considering the errors introduced by the difficulty of modeling a real contoured telephone in the finest details and also the likely errors in experimental measurements, the agreement between the computed and the measured data is reasonably good.

The near fields for this device have also been measured in our laboratory for three different lines parallel to the axis of the helix in the  $z$  direction. For the near-field measurements, we have used a stepper motor equipped with an electric field probe (Narda Model 26089) with a diameter of approximately 4 mm [14]. The comparison in terms of the relative electric fields is within 10%, as shown in Fig. 5.

The second telephone considered uses, instead, a helix-monopole antenna, and its parameters are given as telephone C in Table I. Consistent with the design of this helical antenna, a straight length of 9 mm of metal wire was used to simulate the actual geometry of this antenna. To model the antenna, the helical section has been placed over the metal stack simulating the straight wire connection with the box and a stack of metal cells has been placed over the cells representing the helix to represent the remaining length of the antenna. The measured and computed relative electric fields along one line parallel to the antenna ( $x = 38$  mm) has been plotted in Fig. 6. As for

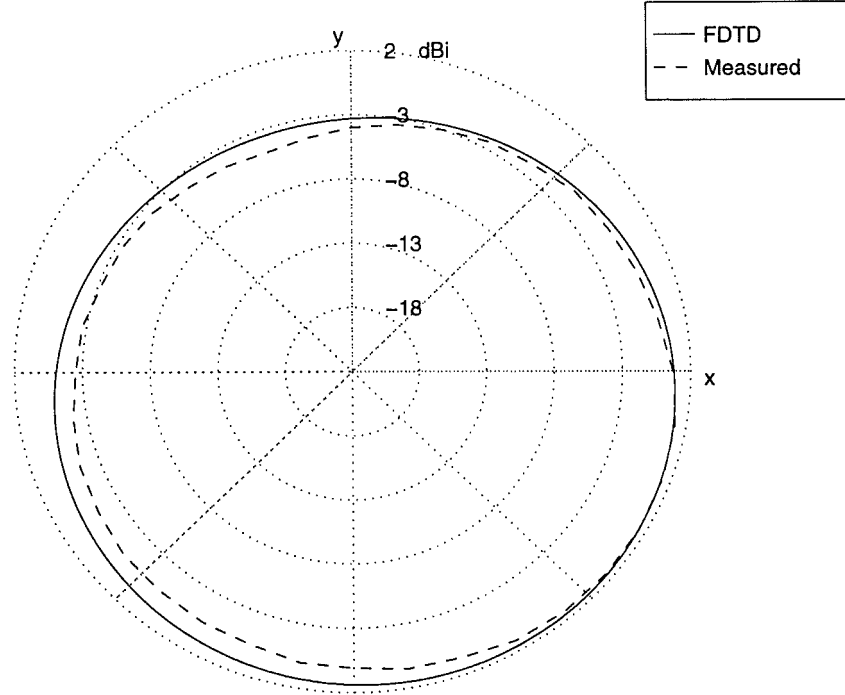


Fig. 4. The computed and measured radiation pattern for an actual cellular telephone using a helix antenna. Box dimensions:  $2.4 \times 5.2 \times 14.7$  cm. The helix has diameter  $D = 4.2$  mm, pitch  $S = 1.4$  mm, length  $L = 1.6$  cm. Frequency: 835 MHz.

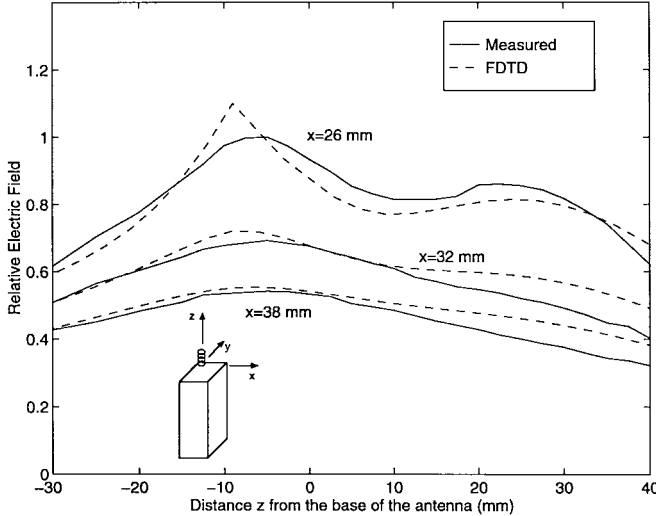


Fig. 5. Comparison between measured and computed relative electric field at distances  $x = 26, 32, 38$  mm from the axis of the antenna for telephone B.

the first helix, here too, the agreement between measured and computed data is within 10%.

The SAR distributions associated with the use of these two telephones (B and C) have also been calculated and compared with the SAR's measured in our laboratory. An MRI-based model of the human head with a resolution of  $1.974 \times 1.974 \times 3$  mm with 15 tissue types identified has been used for the FDTD computations [6], while the experimental head model is a realistically shaped heterogeneous model made of a 5–7-mm-thick saline-laced epoxy shell filled with tissue-simulant materials representing four tissue types (brain, ear, eyes, and muscle) [13]. The dielectric properties used for the

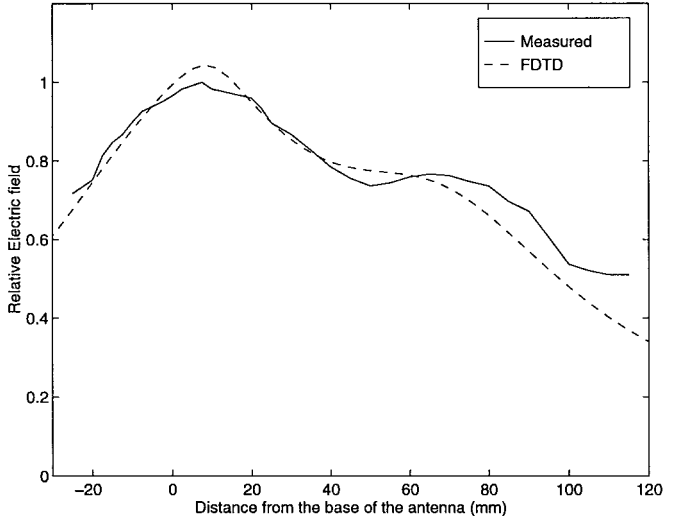


Fig. 6. Comparison between measured and computed relative electric fields at distances  $x = 38$  mm from the axis of the "whip" antenna for telephone C.

various tissues are the same as used in [6]. The comparison is summarized in Table II. As can be seen, the agreement between measured and computed results for the peak 1-g SAR is within 15%.

The radiation pattern for the first of the two telephone in presence of the human head, and with a "hand" modeled as 2/3 muscle grasping the telephone on three sides up to one half of the height of the handset is calculated and compared with that obtained in free-space in Fig. 7. As expected, lower field strengths are calculated in the  $x$ - $y$  plane for directions blocked by the head.

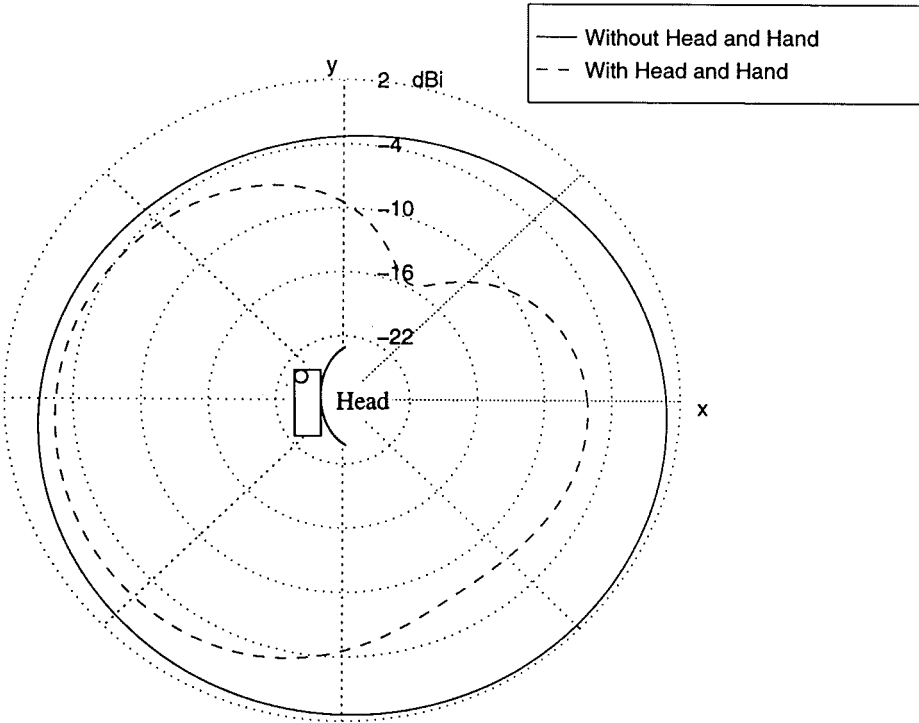


Fig. 7. Computed radiation patterns in the  $x$ - $y$  plane with and without head and hand, for telephone B.

TABLE II

THE MEASURED AND COMPUTED SAR VALUES FOR THE TWO  
CONSIDERED TELEPHONES. TELEPHONE B: 835 MHz, INPUT POWER  
= 600 mW; TELEPHONE C: 1900 MHz, INPUT POWER = 125 mW

	1 g Av. SAR (W/kg) - FDTD -	1 g Av. SAR (W/kg) - Measured -
Telephone B	3.90	4.02
Telephone C	0.15	0.13

## V. CONCLUSION

A novel method to model helical antennas, and generally antennas involving helical components has been presented. The method uses a series of equivalent electric and magnetic sources to reproduce the fields generated by the helix. This method is relatively simple and the FDTD code requires a few simple modifications to the excitation subroutine. Important to note is that no modification of the FDTD grid resolution to represent the helix is needed and modeling of the helix does not require curved metal wires.

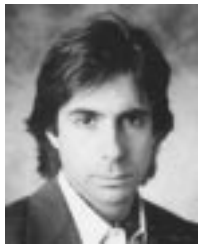
The presented cases show a fairly good agreement between measured and computed data for near-field distributions, far-field radiation patterns, and the SAR deposition in the human head induced by cellular telephones with helical antennas and with helical-monopole antennas that are being increasingly used for commercial cellular telephones.

## ACKNOWLEDGMENT

The authors would like to thank Dr. J. Y. Chen for the preliminary work and Prof. D. Wu for performing the measurements.

## REFERENCES

- [1] J. D. Kraus, *Antennas*, 2nd ed. New York: McGraw-Hill, 1988, ch. 7, pp. 333–338.
- [2] K. S. Yee, “Numerical solution of initial boundary value problems involving Maxwell’s equations,” *IEEE Trans. Antennas Propagat.*, vol. AP-14, pp. 302–307, 1966.
- [3] A. Tafove and M. E. Brodwin, “Numerical solution of steady-state electromagnetic scattering problems using the time-dependent Maxwell’s equations,” *IEEE Trans. Microwave Theory Tech.*, vol. MTT-23, pp. 623–630, 1975.
- [4] A. Tafove, *Computational Electrodynamics: The Finite-Difference Time-Domain Method*. Dedham, MA: Artech House, 1995.
- [5] K. S. Kunz and R. J. Luebbers, *The Finite-Difference Time-Domain Method in Electromagnetics*. Boca Raton, FL: CRC, 1993.
- [6] O. P. Gandhi, G. Lazzi, and C. M. Furse, “Electromagnetic absorption in the human head and neck for mobile telephones at 835 and 1900 MHz,” *IEEE Trans. Microwave Theory Tech.*, vol. 44, pp. 1884–1897, 1996.
- [7] G. Lazzi and O. P. Gandhi, “Realistically tilted and truncated anatomically based models of the human head for dosimetry of mobile telephones,” *IEEE Trans. Electromagn. Compat.*, vol. 39, pp. 55–61, 1997.
- [8] P. J. Dimbylow and S. Mann, “SAR calculations in an anatomically based realistic model of the head for mobile transceivers at 900 MHz and 1.8 GHz,” *Phys. Med. Biol.*, vol. 39, pp. 1537–1553, 1994.
- [9] M. A. Jensen and Y. Rahmat-Samii, “EM interaction of handset antennas and a human in personal communications,” *Proc. IEEE*, vol. 83, pp. 7–17, 1995.
- [10] R. Holland and L. Simpson, “Finite-difference analysis of EMP coupling to thin struts and wires,” *IEEE Trans. Electromagn. Compat.*, vol. EMC-23, pp. 88–97, 1981.
- [11] ANSI/IEEE C95.1-1992, “Standard for safety levels with respect to human exposure to radio frequency electromagnetic fields, 3 kHz to 300 GHz,” IEEE, NY, 1992.
- [12] S. Ramo, J. R. Whinnery, and T. Van Duzer, *Fields and Waves in Communication Electronics*. New York: Wiley, 1967.
- [13] O. P. Gandhi, J. Y. Chen, and D. Wu, “Electromagnetic absorption in the human head for mobile telephones at 835 and 1900 MHz,” in *Proc. Int. Symp. Electromagn. Compat.*, Rome, Italy, Sept. 1994, vol. I, pp. 1–5.
- [14] H. I. Bassen and T. M. Babij, “Experimental techniques and instrumentation,” in *Biological Effects and Medical Applications of Electromagnetic Energy*, O. P. Gandhi, Ed. Englewood Cliffs, NJ: Prentice-Hall, 1990.



**Gianluca Lazzi** (S'94–M'95) was born in Rome, Italy, on April 25, 1970. He received the Dr.Eng. degree in electronics from the University of Rome "La Sapienza," Rome, Italy, and the Ph.D. degree in electrical engineering from the University of Utah, Salt Lake City, UT, in 1994 and 1998, respectively.

He has been a consultant for several companies (1988–1994), a Visiting Researcher at the Italian National Board for New Technologies, Energy, and Environment (ENEA, 1994), a Visiting Researcher at the University of Rome "La Sapienza" (1994–1995), and a Research Associate at the University of Utah (1995). He is the author or coauthor of more than 30 journal articles or international conference presentations on dosimetry and FDTD modeling.

Dr. Lazzi is a member of the New York Academy of the Sciences (NYAS) and the Italian Electrical and Electronic Society (AEI). He is winner of the 1996 International Union of Radio Science (URSI) "Young Scientist Award" and the 1996 "Curtis Carl Johnson Memorial Award" for the best student paper presented at the 18th annual technical meeting of the Bioelectromagnetics Society (BEMS). He is listed in *Who's Who in the World*, *Who's Who in America*, and *Who's Who in Science and Engineering*.



**Om P. Gandhi** (S'57–M'58–SM'65–F'79) received the B.Sc. (honors) degree in physics from Delhi University, Delhi, India, and the M.S.E. and Sc.D. degrees in electrical engineering from the University of Michigan, Ann Arbor.

He is currently a Professor and Chairman of the Department of Electrical Engineering at the University of Utah, Salt Lake City. He is the author or coauthor of several book chapters and journal articles on electromagnetic dosimetry, microwave tubes, and solid-state devices. He also edited *Biological Effects and Medical Applications of Electromagnetic Energy* (Englewood Cliffs, NJ: Prentice-Hall, 1990), and coedited *Electromagnetic Biointeraction* (New York: Plenum, 1989).

Dr. Gandhi received the Distinguished Research Award from the University of Utah for the academic year 1979–1980. He has been President of the Bioelectromagnetics Society (1992–93), co-chairman of the IEEE SCC 28.IV Subcommittee on the RF Safety Standards (1988–1997), and chairman of the IEEE Committee on Man and Radiation (COMAR) for 1980–1982. In 1995, he received the d'Arsonval Medal of the Bioelectromagnetics Society for pioneering contributions to the field of bioelectromagnetics. He is listed in *Who's Who in the World*, *Who's Who in America*, *Who's Who in Engineering*, and *Who's Who in Technology Today*.